An Insight into the Dynamical Behaviour of the Swing Equation

ANASTASIA SOFRONIOU, BHAIRAVI PREMNATH, KEVIN JAGADISSEN MUNISAMI
School of Computing and Engineering
University of West London
St. Mary's Road, W5 5RF
UNITED KINGDOM

Abstract: Motivated by the nonlinear dynamics of mathematical models encountered in power systems, an investigation into the dynamical behaviour of the swing equation is carried out. This paper examines analytically and numerically the development of oscillatory periodic solutions, whereby increases of the control parameter, lead to a cascade of period doubling bifurcations, before eventually loss in stability is exhibited and effective forerunners to chaos revealed. Gaining an understanding on the dynamical behaviour of the system can help to produce a deeper insight of the bifurcations entailed, with the appearance of the triggered sequence of the first period doubling's acting as precursors of imminent danger and difficult operations of a practical system.

Key-Words: nonlinear dynamics, swing equation, chaos

Received: September 27, 2022. Revised: November 16, 2022. Accepted: December 15, 2022. Published: January 25, 2023.

1 Introduction

Stability in a power system is closely tied to the concept of disturbances, which are sudden or sequential changes to the system's parameters or operating quantities. Even a small disturbance can have an interesting and rich effect in terms of the dynamics of a system. Linearising the equations that represent a system [1], undertaking eigenvalue and frequency response methods can be employed to study the stability of the system [2, 3].

In this study, a single degree of freedom system is considered that will allow for the study of nonlinear dynamics to be examined and to acknowledge even chaotic attractors. This study focuses on the nonlinear aspect of solving a system using methods such as perturbation techniques and nonlinear methods. Initially in this study, an infinite busbar is represented with the assumption of constant voltage and frequency. A busbar system is a metallic strip/bar used for high-current power distribution. It is usually used in panel boards, switchgear, and home circuits. In general, the busbars are uninsulated and receive support from the air by insulated pillars, allowing for enough cooling for the conductors [4]. If a classical representation is considered, that is with a fixed voltage behind a transient reactance, then the busbar system is reduced to a second-order differential equation but with constant coefficients. As this resulting equation does not offer much useful or novel information about the response of the system, the analogous swing equation is considered here within, which includes parametric and external excitations allowing for the techniques of perturbation theory to be employed under this new formulation of the extended busbar system [5, 6].

This newly formulated swing equation will be analysed analytically and numerically to obtain a better understanding of the stability of the model.

1.1 Brief Literature Review

A power system is stable at a particular operating condition when it is able to maintain a steady state. When the system experiences a small disturbance, it is able to return to its pre-disturbance operating conditions or achieve a steady state once again. However, in the event of a large disturbance, the equations that describe the system's behavior can no longer be linearised, and it becomes necessary to use numerical simulation techniques based on geometric methods to analyze the system's behavior, which is now considered to be a part of nonlinear dynamics [6, 7]. The focus of this paper is the nonlinear aspect of systems which can be addressed through various dynamical and perturbation techniques [8, 9]. Researchers have studied the swing equation which showed the rotor of the machine's motion [6, 7, 10]. Although power systems have been studied for quite some time now, the growth

of the topic is tremendous. The power system in electric applications has seen ongoing development in many areas [11]. With this growth, the conservation of energy and renewing the existing energy have been under the radar by many institutions. To help with the environmental concerns the power systems must be studied further, and new techniques should be introduced [12].

The swing equation which is studied initially in this research work will play a vital part in the analysis of the dynamics of a power system [13]. It does exhibit similar characteristics as other power systems, but it is imperative to analyse it first in detail for a better understanding of the concepts. Recent research has found that the generalised form of the swing equation also helps with understanding transient stability in power-electronic power systems [14]. During any slight disturbance, the rotor of the machine will show some motion with respect to the synchronously rotating air gap. This in turn starts a relative motion allowing for the swing equation to describe and model this relative motion [15, 16]. Although Tamura et al. [10] initiated the quasi-infinite busbar which is formulated in phase and magnitude, Hamdan and Nayfeh [3, 8] improved the idea to have quadratic and cubic nonlinearities. This helps in applying techniques such as perturbation analysis to the single-machine-quasi-infinite busbar system.

As it is well known, bifurcation occurs when a small change to a parameter value of a system causes a change in the behaviour whether this is a topological or qualitative change occurring in both discrete and continuous systems. A bifurcation has significant effects on power systems, including oscillation and voltage collapse [17, 18]. Eigenvalue analysis may be further utilised to consider stability and to determine the nature of the system [19]. Bifurcations can be studied using both mathematical models and computer simulations involving oscillators [20]. Some authors have pointed out the limitations of using physical oscillators for this purpose and have suggested computer algorithms as an alternative for more accurate and efficient analysis of bifurcations. Matlab software, specifically the packages MATCONT and CLMATCONT, can be used to analyse dynamical systems with bifurcations. In a study [21, 22], the unique nature of a parametrically pressurized system was characterized using a pinched cylinder, and the mechanism of symmetry-breaking pitchfork bifurcation was examined. It has been shown that the stability and behavior of the swing equation can be affected by various factors, and that increasing the time delay can cause limit cycle branches to move and combine through bifurcations [23].

In [24, 25] bifurcation analysis is employed to estimate the boundary of the chaotic precursors of a parametrically excited pendulum system, considering the effect of a bias term inclusion in the model that breaks the symmetry of the system, gaining deeper insights into bifurcations entailed with the purpose of growing a higher realisation for any unique problem. The authors also explain that the easy uneven equation of movement proposed in the study ends in diverse nonlinear phenomena, inclusive of cascades of period doubling bifurcations, which had been tested and compared with different models.

2 Methodology

2.1 Analytical Work

The swing equation studied here depicts the motion of rotor of machine as reproduced below as Figure 1 [26].

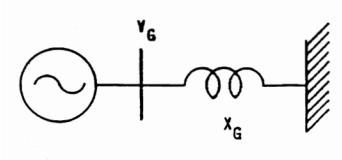

Fig. 1: Swing equation describing the motion of the rotor of the machine. Figure reproduced from [26].

Considering the damping term, the swing equation that describes the motion of the rotor of the machine employed in this study is as follows [6, 7, 10],

$$\frac{2H}{\omega_R}\frac{d^2\theta}{dt^2} + D\frac{d\theta}{dt} = P_m - \frac{V_G V_B}{X_G}\sin(\theta - \theta_B) \quad (1)$$

$$V_{\mathrm{B}} = V_{B0} + V_{\mathrm{B1}}\cos(\Omega t + \phi_v) \quad (2)$$

$$\theta_B = \theta_{B0} + \theta_{B1}\cos(\Omega t + \phi_0) \quad (3)$$

with
$\omega_R = Constant\ angular\ velocity$,
H= Inertia,
D= Damping,
$\mathrm{P}_m = Mechanical\ Power$,
$\mathrm{V}_G = Voltage\ of\ machine$,
$\mathrm{X}_G = Transient\ Reactance$,
$\mathrm{V}_B = Voltage\ of\ bus$,

$\theta_B = phase\ of\ bus.$

V_{B1} *and* θ_{B1} *magnitudes assumed to be small.*

Mathematical analysis is performed on this equation for further investigation whereby algebraic techniques, Taylor expansion and substitution are undertaken so as to obtain a final equation that will be used for the perturbation analysis.

Allowing consideration for the transformations,

$$\theta - \theta_B = \delta_0 + \eta \tag{4}$$

$$\delta_0 = \theta_0 - \theta_{B0} \tag{5}$$

$$\eta = \Delta\theta - \theta_{B1}\cos(\omega t + \phi_0) \tag{6}$$

equation (4) becomes,

$$\sin(\theta - \theta_B) = \sin(\delta_0 + \eta) \tag{7}$$

with first differential and second differential equations of (4) being substituted into equations (1), (2) and (3) to derive the modified swing equation with excitation to:

$$\frac{d^2\eta}{dt^2} + \frac{\omega_R D}{2H}\frac{d\eta}{dt} + K\eta = \alpha_2\eta^2 + \alpha_3\eta^3 + \mathrm{G}_1\eta\cos(\Omega t + \phi_v) + G_2\eta^2\cos(\Omega t + \phi_v) + G_3\eta^3\cos(\Omega t + \phi_v) + Q_1\cos(\Omega t + \phi_\theta) + Q_2\sin(\Omega t + \phi_\theta) + Q_3\cos(\Omega t + \phi_v) \tag{8}$$

and with,

$$\alpha_2 = \frac{1}{2}K\tan\delta_0, \qquad \alpha_3 = \frac{1}{6}K,$$

$$G_1 = \frac{-V_{B1}}{V_{B0}}K, \qquad G_2 = \frac{-V_{B1}}{2V_{B0}}K\tan\delta_0,$$

$$G_3 = \frac{-V_{B1}}{6V_{B0}}K,$$

$$Q_1 = \Omega^2\theta_{B1}, \qquad Q_2 = \frac{\Omega D\omega_R\theta_{B1}}{2H},$$

$$Q_3 = \frac{-V_{B1}}{V_{B0}}K\tan\delta_0,$$

$$K = \frac{V_G V_{B0}\omega_R\cos\delta_0}{2HX_G},$$

here

$\mathrm{Q}\cos(\Omega t + \phi_e) = Q_1\cos(\Omega t + \phi_\theta) + \mathrm{Q}_2\sin(\Omega t + \phi_\theta) + Q_3\cos(\Omega t + \phi_v)$,

equation (8) reduces to,

$$\frac{d^2\eta}{dt^2} + \frac{\omega_R D}{2H}\frac{d\eta}{dt} + K\eta = \alpha_2\eta^2 + \alpha_3\eta^3 + \mathrm{G}_1\eta\cos(\Omega t + \phi_v) + G_2\eta^2\cos(\Omega t + \phi_v) + G_3\eta^3\cos(\Omega t + \phi_v) + Q\cos(\Omega t + \phi_e). \tag{8a}$$

Perturbation Analysis

Initially, the focus of the analysis is on primary resonance. To study this, a technique called multiple scales is used to find a uniform solution for equation (8a). A small, dimensionless parameter ε is introduced to account for the effects of damping, nonlinearities, and the excitation frequency, which occur in a specific order.

Letting

$$\eta = O(\varepsilon), \quad \frac{\omega_R D}{2H} = O\left(\varepsilon^2\right)$$

and

$$V_{B1} = O(\varepsilon^3)\ and\ \theta_{B1} = O(\varepsilon^3),$$

then the final equation from the swing equation derivation above has the following coefficients,

$$G_1 = \varepsilon^3 g_1,\ G_2 = \varepsilon^3 g_2,\ G_3 = \varepsilon^3 g_3$$

$$Q = \varepsilon^3 q.$$

Also, considering the equation with detuning parameter σ.

$$\omega_0^2 = \Omega^2 + \mathcal{E}^2\sigma$$

to allow for the derived final swing equation (8a) to be re-written as,

$$\ddot{\eta} + 2\varepsilon^2\mu\dot{\eta} + (\Omega^2 + \mathcal{E}^2\sigma)\eta = \alpha_2\eta^2 + \alpha_3\eta^3 + \varepsilon^3 g_1\eta\cos(\Omega t + \phi_v) + \varepsilon^3 g_2\eta^2\cos(\Omega t + \phi_v) + \varepsilon^3 g_3\eta^3\cos(\Omega t + \phi_v) + \varepsilon^3 q\cos(\Omega t + \phi_e) \tag{9}$$

The solution to this above equation is of the form:

$$\eta(t;\varepsilon) \;=\; \varepsilon\eta_1(T_0,T_1,\;T_2) \;+\; \varepsilon^2\eta_2(T_0,T_1,\;T_2) \;+\; \varepsilon^3\eta_3(T_0,T_1,\;T_2) + ... \tag{10}$$

where T_0 is a fast scale describing motions of frequencies and T_1, T_2 are slow scales describing amplitude variation [26].

The first derivative of this equation will be,

$$\frac{d}{dt} \;=\; D_0 \;+\varepsilon D_1 + \varepsilon^2 D_2 + ... \tag{11}$$

The second derivative of the equation is,

$$\frac{d^2}{dt^2} \;=\; D_O^2 + 2_0 D_1 + \varepsilon^2(2D_0D_2 + D_1^2) + ... \tag{12}$$

where

$$D_n = \frac{\partial}{\partial T_n}.$$

Equation (10) can be rewritten as;

$$\eta \;=\; \varepsilon\eta_1 + \varepsilon^2\eta_2 + \varepsilon^3\eta_3 + ... \tag{13}$$

Finding the first derivative with respect to t for equation (13) and substituting equation (11) gives,

$$\eta\;(D_0 + \;\varepsilon D_1 \;+\; \varepsilon^2 D_2 + ...) \;=\; \varepsilon\eta_1(D_0 + \varepsilon D_1 \;+\; \varepsilon^2 D_2 + ...) + \;\varepsilon^2\eta_2(D_0 + \;\varepsilon D_1 \;+ \varepsilon^2 D_2 + ...) \;+\; \varepsilon^3\eta_3 + (D_0 + \;\varepsilon D_1 \;+\; \varepsilon^2 D_2 + ...) \tag{11a}$$

Differentiating for the second derivative with respect to t for equation (13) and substituting equation (12) to obtain,

$$\eta\;(D_0^2 \;+ 2\varepsilon D_0D_1 \;+\; \varepsilon^2(2D_0D_2 + \;D_1^2) + ...) = \;\varepsilon\eta_1(D_0^2 + 2\varepsilon D_0D_1 + \;\varepsilon^2(2D_0D_2 + \;D_1^2) + ...) + \;\varepsilon^2\eta_2(D_0^2 + 2\varepsilon D_0D_1 + \;\varepsilon^2(2D_0D_2 + \;D_1^2) + ...) \;+\; \varepsilon^3\eta_3(D_0^2 + 2\varepsilon D_0D_1 + \;\varepsilon^2(2D_0D_2 + \;D_1^2) + ...) \tag{11b}$$

Substituting equations (11a), (11b) and (13) into equation (9) and comparing coefficients of ε gives,

$$\varepsilon^1/: \;\; \eta_1 D_0^2 + \eta_1\Omega^2 \;=\; 0 \tag{14}$$

$$\varepsilon^2/: \;\; \eta_1 D_0^2 + \;\eta_2\Omega^2 + 2D_0D_1\eta_1 \;=\; \alpha_2\eta_1^2 \tag{15}$$

$$\varepsilon^3\;/: \;\; D_0^2\eta_3 + \;2D_0D_1\eta_2 \;+\; (D_1^2 \;+\; 2D_0D_2)\eta_1 + \;2_0\eta_1 \;+\; \Omega^2\eta_3 \;+\; \sigma\eta_1 = \;2\alpha_2\eta_1\eta_2 + \;\alpha_3\eta_1^3 \;+ q\cos(\Omega t + \;\phi_e) \tag{16}$$

From equations (14), (15) and (16) it can be seen that the parametric terms do not have key effects on the system. Hence only the external forcing term remains [26].

The solution to equation (14) is of the form:

$$\eta_1 \;=\; A(T_1,\;T_2)\,e^{i\Omega T_0} + \bar{A}(T_1,\;T_2)\,e^{-i\Omega T_0} \tag{17}$$

where A is an undetermined function. Given that

$$D_n = \;\frac{\partial}{\partial T_n},\; D_0 = \;\frac{\partial}{\partial T_0}$$

by integration,

$$T_0 \;= \frac{1}{D_0}.$$

Substituting equation (17) into (15),

$$\eta_2 D_0^2 \;+\; \;\eta_2\Omega^2 \;=\; -\;2D_0D_1(A(T_1,\;T_2)\;e^{i\Omega T_0} + \bar{A}(\mathrm{T}_1,\;T_2)\;e^{-i\Omega\;\mathrm{T}_0} + \alpha_2(A(T_1,\;T_2)\;e^{i\Omega T_0} + \bar{A}(\mathrm{T}_1,\;T_2)\;e^{-i\Omega\;\mathrm{T}_0})^2$$

and expanding the brackets,

$$\eta_2 D_0^2 \;+\; \;\eta_2\Omega^2 \;=\; -\;2D_0D_1A(T_1,\;T_2)\;e^{i\Omega T_0}$$

$$-\;2\mathrm{D}_0D_1\;\bar{A}(T_1,\;T_2)\;e^{-i\Omega T_0} + \;\alpha_2((A^2\;e^{2i\Omega T_0} + \bar{A}^2\;e^{-2i}\Omega\;\mathrm{T}_0 \;+\; 2A\bar{A}).$$

Due to $D_0 = \;\frac{\partial}{\partial T_0}$ and

$$\frac{\partial(2D_0D_1A\;e^{i\Omega T_0})}{\partial T_0} \;=\; 2i\Omega D_1A\;e^{i\Omega T_0}$$

$$\frac{\partial(2D_0D_1\bar{A}\;e^{-i\Omega T_0})}{\partial T_0} \;=\; -2i\Omega D_1\bar{A}e^{-i\Omega T_0}$$

substituting into the equation and rearranging leads to,

$$\eta_2 D_0^2 \;+\; \;\eta_2\Omega^2 \;=\; -\;2i\Omega D_1A\;e^{i\Omega T_0} + \;\alpha_2(A^2\;e^{2i\Omega T_0} \;+\; \bar{A}^2\;e^{-2i\Omega T_0}\;) + \bar{c} \tag{18}$$

where $\bar{c}$ is the complex conjugate.In this equation $D_1 A = 0$, to avoid secular terms η_2 and hence $A = A(T_2)$ so that replacing equation (14) into (18) and simplifying,

$$\eta_2 = -\frac{\alpha_2(A^2\ e^{2i\Omega T_0}\ )}{3\Omega^2} - \frac{\alpha_2(\bar{A}^2\ e^{-2i\Omega T_0}\ )}{3\Omega^2} + \frac{2\alpha_2 A\bar{A}}{\Omega^2} \quad (19)$$

which is also echoed in [26].

Replacing equations (17) and (19) into equation (16),

$$\mathrm{D}_0^2\eta_3 + 2D_0D_1(-\tfrac{\alpha_2(A^2\ e^{2i\Omega T_0}\ )}{3\Omega^2} - \tfrac{\alpha_2(\bar{A}^2\ e^{-2i\Omega T_0}\ )}{3\Omega^2} + \tfrac{2\alpha_2 A\bar{A}}{\Omega^2}\ ) + (D_1^2 + 2D_0D_2)\ (A\ e^{i\Omega T_0} + \bar{A}e^{-i\Omega T_0}) + 2\mu D_0(Ae^{i\Omega T_0} + \bar{A}\ e^{-i\Omega T_0}\ ) + \Omega^2\eta_3 + \sigma(Ae^{i\Omega T_0} + \bar{A}e^{-i\Omega T_0}) = 2\alpha_2(A\ e^{i\Omega T_0} + \bar{A}e^{-i\Omega T_0}\ )(-\tfrac{\alpha_2(A^2\ e^{2i\Omega T_0}\ )}{3\Omega^2} - \tfrac{\alpha_2(\bar{A}^2\ e^{-2i\Omega T_0}\ )}{3\Omega^2} + \tfrac{2\alpha_2 A\bar{A}}{\Omega^2}\ ) + \alpha_3(Ae^{i\Omega T_0} + \bar{A}\ e^{-i\Omega T_0})^3 + q\cos(\Omega t + \phi_e)$$

and importing the cubic bracket separately of,

$$\alpha_3(Ae^{i\Omega T_0} + \bar{A}\ e^{-i\Omega T_0})^3 = \alpha_3 A^3 e^{3i\Omega T_0} + 3\alpha_3 A^2\bar{A}e^{i\Omega T_0} + 3\alpha_3 A\bar{A}^2\bar{A}e^{i\Omega T_0} + \alpha_3\bar{A}^3e^{3i\Omega T_0},$$

eliminating terms that lead to secular terms and $D_1 A = 0$ then,

$$2i\mu\Omega\ (A' + \mu A) + -\frac{1}{2}ge^{i\phi} + 8\alpha_e A^2\bar{A} = 0 \quad (20)$$

where

$$\alpha_e = -\frac{3}{8}\alpha_3 - \frac{5\alpha_2^2}{12\Omega^2}.$$

Expressing A in polar form,

$$A = \frac{1}{2}\ ae^{-i(\beta + \phi_e)} \quad (21)$$

and substituting equation (21) into equation (20) gives,

$$2i\mu\Omega\ (\frac{1}{2}\ a'e^{-i(\beta+\ \phi_e)} + \mu(\frac{1}{2}\ ae^{-i(\beta+\ \phi_e)})) + \sigma(\tfrac{1}{2}ae^{-i(\beta+\ \phi_e)}) - \tfrac{1}{2}ge^{i\phi} + 8\alpha_e(\tfrac{1}{2}\ ae^{-i(\beta+\ \phi_e)})^2(\tfrac{1}{2}\ a'e^{-i(\beta+\ \phi_e)}) = 0.$$

Separating real and imaginary parts,

$$\Omega(a' + \mu a) + \frac{1}{2}q\sin\beta = 0 \quad (22)$$

$$-\Omega a\beta' + \alpha_e a^3 - \frac{1}{2}q\cos\beta + \frac{1}{2} = 0. \quad (23)$$

Equation (21) can also be written in the form:

$$A = \frac{1}{2}a\ cos(\beta + \phi_e)$$

Substituting A and its conjugate into equation (17) leads to:

$$\eta_1 = a\ cos(2\Omega t + \beta + \phi_e)$$

Similarly replacing into equation (19) gives:

$$\eta_2 = \frac{\alpha_2 a^2}{2\Omega^2} - \frac{\alpha_2 a^2}{6\Omega^2}\ cos\ (2\Omega t + 2\beta + 2\phi_e)$$

Substituting the above to derivations for η_1 and η_2 in equation (10) to obtain the second approximation,

$$\eta = \varepsilon a\ \cos(\Omega t + \beta + \phi_e) + \frac{\varepsilon^2 a^2\alpha_2}{6\Omega^2}\ [3 - \cos(2\Omega t + 2\beta + 2\phi_e)] + ... \quad (24)$$

Setting $\varepsilon = 1$ and letting " a" be the perturbation parameter, using equation (24), equation (6) maybe rewritten as,

$$\Delta\theta = \theta_{B1}\ \cos(\Omega t + \phi_\theta) + a\ \cos(\Omega t + \beta + \phi_e) + \frac{a^2\alpha_2}{6\Omega^2}\ (3 - \cos(2\Omega t + 2\beta + 2\phi_e)) + ...$$

with $\frac{a^2\alpha_2}{2\Omega^2}$ defined as the drift term, which because of its quadratic nonlinearity the oscillatory motion is not centered as seen also in [26].

To understand the character of equations (22) and (23), fixed points are found in align with $a' = \beta' = 0$ to reduce to:

$$\mu a = -\frac{q\sin\beta}{2\Omega} \quad (24a)$$

$$\frac{a\sigma}{2\Omega} + \frac{\alpha_e a^3}{\Omega} = \frac{q\cos\beta}{2\Omega} \quad (24b)$$

Squaring and adding equations (24a) and (24b) will give,

$$\mu^2 + (\frac{\sigma}{2\Omega} + \frac{\alpha_e a^2}{\Omega})^2 = \frac{q^2}{4\Omega^2 a^2} \quad (25)$$

which is an implicit equation for α (amplitude) as a function of σ (the tuning parameter).

In order to compare the analytical results with the numerical simulations for the case of primary resonance, the following figure, Figure 2, presents phase portraits and time histories when $\Omega = 8.61$ rad/sec. Runge-Kutta and Newton Raphson method were both employed for the simulation of the perturbation analysis and both compared with its numerical counterpart, to conclude that the Newton Raphson algorithm gives a better approximation to the numerical solution. The calculated numerical error of the Runge-Kutta method versus the Newton Raphson technique compared to the actual simulation error was 0.0884 and 0.0747 respectively, exemplifying that the Newton Raphson method is a more appropriate fit due to the smaller error value.

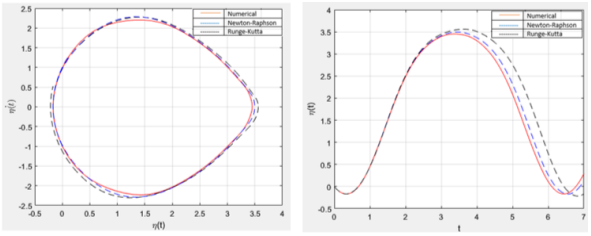

Fig. 2: Perturbed solution employing Runge-Kutta and Neton Raphson algorithms in comparison to numerical simulations for the case of primary resonance in the phase plane and time history for $\Omega = 8.61$ rad/sec.

2.2 Numerical Analysis

Graphical Representation

The free undamped oscillation of the machine is given by,

$$\frac{d^2\theta}{dt^2} - \frac{\omega_R P_m}{2H} + \frac{\omega_R V_G V_{B0}}{2HX_G} \sin(\theta - \theta_{B0}) = 0.$$

When the damping term is introduced into the system, the phase plane alters diagrammatically. Matlab was employed to numerically determine the phase space plots for the undamped and damped oscillator.

Figures 3 and 4 pictorially show the phase portraits for a variation of c values, c being the value of the solution of the differential equation. The

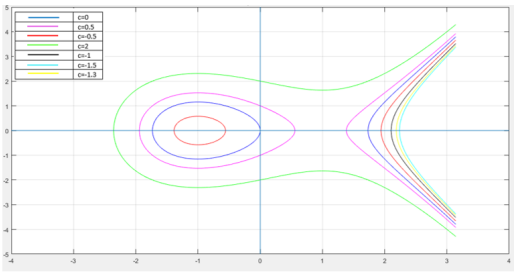

Fig. 3: Phase portrait: undamped oscillation for the different stated c values.

damped oscillation is given by the following equation, with D representing the damping term,

$$\frac{d^2\theta}{dt^2} + \frac{\omega_R D}{2H}\frac{d\theta}{dt} - \frac{\omega_R P_m}{2H} + \frac{\omega_R V_G V_{B0}}{2HX_G} \sin(\theta - \theta_{B0}) = 0$$

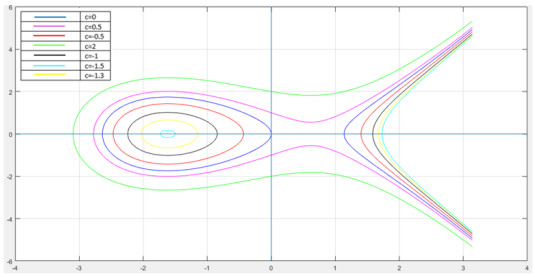

Fig. 4: Phase portrait: damped oscillation for the different stated c values.

The phase portraits of free oscillations show saddle point separating its closed orbits from the trajectories which go off to infinity [6, 26, 27].

The equations (1), (2) and (3) were configured and solved using the fourth-order Runge-Kutta method in Matlab, focusing on the effect of varying the excitation frequency Ω.

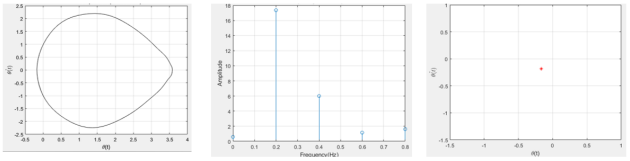

Fig. 5: Phase portrait, frequency-domain plot and Poincaré map when $\Omega = 8.61$ rad/sec.

Figures 5, 6, 7, 8 and 9 were obtained by plotting the phase portraits, frequency-domain plots, and Poincaré maps when this excitation frequency is varied in the swing equation (1). As

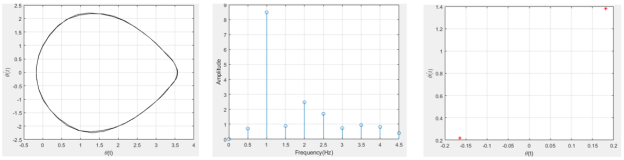

Fig. 6: Phase portrait, frequency-domain plot and Poincaré map when $\Omega = 8.43$ rad/sec.

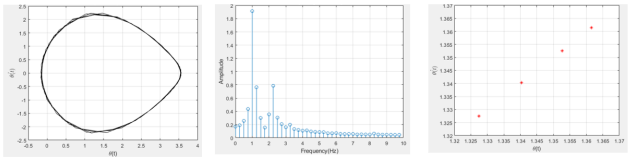

Fig. 7: Phase portrait, frequency-domain plot and Poincaré map when $\Omega = 8.282$ rad/sec.

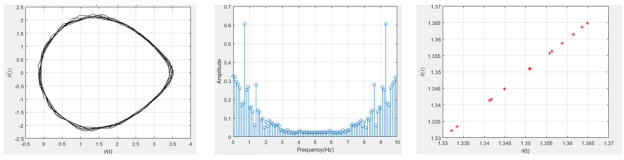

Fig. 8: Phase portrait, frequency-domain plot and Poincaré map when $\Omega = 8.275$ rad/sec.

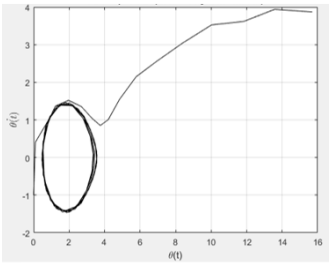

Fig. 9: Phase portrait (loss of synchronism) when $\Omega = 8.2601$ rad/sec.

it is decreased the system begins to lose stability and cascades towards chaos. Each plot represents the different period doubling and how the system loses its synchronism. Figure 5 shows that there exists only one steady-state attractor when there is a large Ω, $\Omega = 8.61$ rad/sec. The phase orbit has a closed form and is a period-one attractor. This can be verified using the frequency-domain plot and the Poincaré map.

As the value of Ω is decreased it can be observed that the graphs undergo dynamical transformations including period-doubling solutions and eventually as Ω is decreased to further around $\Omega = 8.2601$ rad/sec a chaotic attractor is exhibited as exemplified in Figure 9.

The bifurcation diagram presented as Figure 10, was constructed by solving the swing equation for a specific value of $\Omega = 8.27$ rad/sec and by numerical time integration using the classical fourth order Runge-Kutta algorithm. The forcing r value is incremented slightly and time integration continues plotting the maximum amplitude of the oscillatory solution versus r,

$$r = \frac{V_G V_B}{X_G} \sin(\theta - \theta_B).$$

Figure 10 indicates the initial period doubling occurrence just before r = 0.9, also justified by the Poincaré maps of Figure 11 and at around r approximately 2.36, the first period doubling in a sequence of period doubles is exhibited leading to chaotic behaviour. This numerical analysis shows that the swing equation moves towards loss of synchronisation as the value of r is increased.

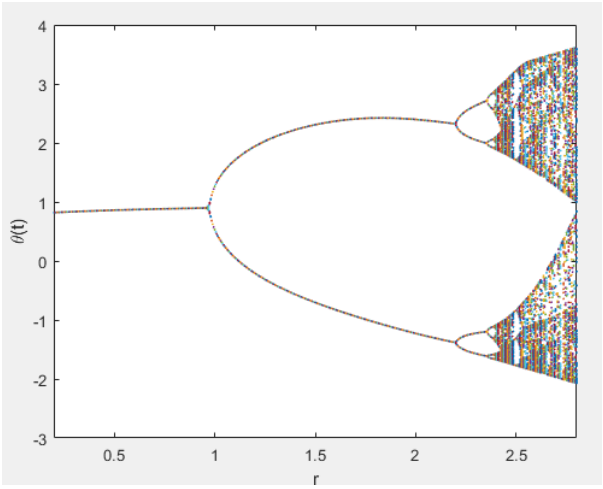

Fig. 10: Bifurcation diagram when r value is varied and constant $\Omega = 8.27$ rad/sec.

The corresponding Poincaré maps are plotted as shown below, Figure 11. They clearly depict the points where period doubling occurs and how as r is increased the phenomenon of chaos is verified.

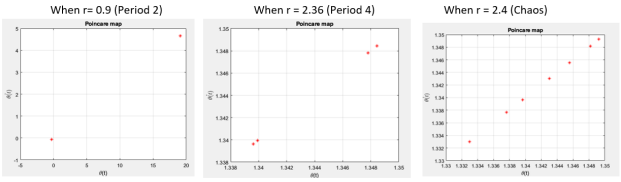

Fig. 11: Poincaré maps for the different r values.

It is observed that at approximately $r > 2.4$, the chaotic region has commenced where the Lyapunov exponent generally takes positive values.

This behaviour is depicted and presented as Figure 12, where it is the case when two nearby points, initially separated by an infinitesimal distance, typically diverge from each other over time and this is quantitatively measured by the Lyapunov exponents. The bifurcation diagram of Figure 10, also verifies this behaviour, where at approximately the same value of r, the cascade of period doubling sequence leads to chaos such that is suffices to say that a chaotic attractor can be identified by a positive Lyapunov exponent.

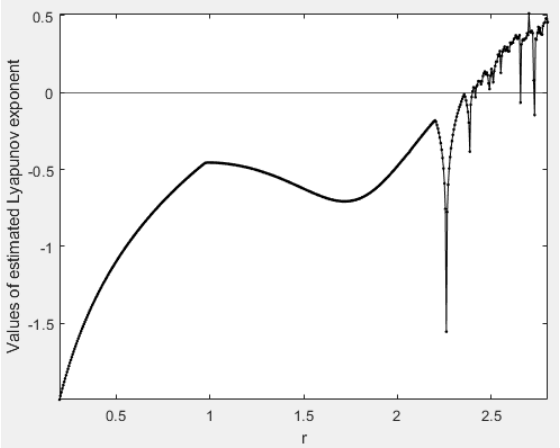

Fig. 12: Lyapunov exponents as r is varied.

3 Discussion and Conclusion

This paper highlights the dynamical behaviour of the swing equation as control parameters are varied. The entailed work provides analytical methods, specifically perturbation techniques which are compared with the numerical simulation to verify the validity of the perturbed solution for the case of primary resonance.

The swing equation is used to predict the behavior of the system under various conditions, such as changes in load. This information is used by power system operators to maintain the stability and reliability of the system. It may be used in the design and analysis of control systems for power systems, such as automatic generation control and load frequency control, preventing blackouts and even more so, catastrophic effects.

The numerical analysis incorporating a numerically constructed bifurcation diagram, Lyapunov exponents, phase portrait, frequency domain plots and Poincaré maps, all confirm that an appearance of the first period doubling in its sequence triggers chaos, and should be regarded as a precursor of the imminent danger and difficult operations of a practical system. It is important to note that the bifurcation diagrams do examine pre-chaotic or post-chaotic changes in a dynamical system under different parameter variations and whilst period doubling is the most recognised scenario for chaotic behaviour, there are also other scenarios to reach this phenomenon, such as intermittency or the break-up of the quasi periodic torus structure. It is beneficial however, to identify a pre-chaos pattern of motion in order to offer a better understanding of the under study chaotic physical phenomenon. The aim of this paper is to compliment current literature of this model utilised in power systems, yet gaining a better understanding of the underlying swing equation.

References:

[1] IEEE Task Force, "Proposed terms and definitions for power system Stability," /EEE Trans. Power Appar. Syst., Vol. PAS-101, 1982, pp. 1894-1898.

[2] F. M. Hughes and A. M. A. Hamdan, "Design of turboalternator excitation controllers using multivariable frequency response methods." Proceedings of the IEE, Vol. 123,1976, pp. 901-905.

[3] H. M. A. Hamdan, A. M. A. Hamdan, and B. Kahhaleh, "Damping of power system oscillations using a current feedback signal," Proceedings of the IEE, Vol. 136, Part C,1989, pp. 137-144.

[4] Bao, Y.J., Cheng, K.W.E., Ding, K. and Wang, D.H., 2013, December. The study on the busbar system and its fault analysis. In 2013 5th International Conference on Power Electronics Systems and Applications (PESA) (pp. 1-7). IEEE.

[5] P. Berge, Y. Pomeau, and C. Vidal, Order Within Chaos, 1984, Wiley-Interscience, New York.

[6] P.M. Anderson and A. A. Fouad, Power System Control and Stability , 1977, The lowa State University Press.

[7] Pai, Power System Stability-Analysis by the Direct Method of Lyapunov,1981, North Holland, New York.

[8] A. H. Nayfeh, Perturbation Methods , 1973, Wiley-Interscience, New York.

[9] A. H. Nayfeh, Introduction to Perturbation Techniques , 1981, Wiley-Interscience, New York.

[10] T. Tamura and Y. Yorino, "Possibility of Auto- and Hetero- Parametric Resonances in Power Systems and their Relationship with Long-Term Dynamics," /EEE Transactions on Power Systems, Vol. PWRS-2, 1987 pp. 890-897.

[11] Kothari, D.P., March. Power system optimization. In 2012 2nd National conference on computational intelligence and signal processing (CISP) ,2012,(pp. 18-21). IEEE.

[12] M. Zhao, X. Yuan, J. Hu, and Y. Yan, "Voltage dynamics of current control time-scale in a VSC-connected weak grid," IEEE Trans. Power Syst. 31, 2015, 2925–2937.

[13] Qiu, Q., Ma, R., Kurths, J. and Zhan, M. Swing equation in power systems: Approximate analytical solution and bifurcation curve estimate. Chaos: An Interdisciplinary Journal of Nonlinear Science, 30(1), 2020, p.013110.

[14] Ma, R., Li, J., Kurths, J., Cheng, S. and Zhan, M. Generalized Swing Equation and Transient Synchronous Stability With PLL-Based VSC. IEEE Transactions on Energy Conversion, 37(2),2021, pp.1428-1441.

[15] Padhi, S., and B. P. Mishra. "Solution of swing equation for transient stability analysis in dual-machine system.",2015, IOSR Journal of Engineering 5.

[16] David Crawford, J. 1989, Introduction to bifurcation theory.

[17] Chiang, H. D. et al. 'Chaos in a simple power system', IEEE Transactions on Power Systems, 8(4), 1993,pp. 1407–1417. doi: 10.1109/59.260940.

[18] Chitnis, N., Cushing, J. M. and Hyman, J. M. 'Bifurcation analysis of a mathematical model for malaria transmission', SIAM Journal on Applied Mathematics, 67(1), 2006, pp. 24–45. doi: 10.1137/050638941.

[19] Crandall, M. G. and Rabinowitz+, P. H. 1971, Bifurcation from Simple Eigenvalues, Journal of Functional Analysis.

[20] Sieber, J. and Krauskopf, B. 'Control based bifurcation analysis for experiments', Nonlinear Dynamics, 51(3),2008, pp. 365–377. doi: 10.1007/s11071-007-9217-2.

[21] Miles, John W. "Nonlinear faraday resonance." Journal of Fluid Mechanics 146 (1984): 285-302.

[22] Bishop, S. R., Sofroniou, A. and Shi, P. 'Symmetry-breaking in the response of the parametrically excited pendulum model', Chaos, Solitons and Fractals, 25(2), 2005,pp. 257–264. doi: 10.1016/j.chaos.2004.11.005.

[23] Scholl, Tessina H., Lutz Gröll, and Veit Hagenmeyer. "Time delay in the swing equation: A variety of bifurcations." Chaos: An Interdisciplinary Journal of Nonlinear Science 29, no. 12 (2019): 123118.

[24] Sofroniou, A. and Bishop, S. 'Dynamics of a Parametrically Excited System with Two Forcing Terms', Mathematics, 2(3), 2014, pp. 172–195. doi: 10.3390/math2030172.

[25] Sofroniou, Anastasia. The parametrically excited pendulum system and applications to ship dynamics, 2006 University of London, University College London (United Kingdom).

[26] Nayfeh, Mahir Ali. "Nonlinear dynamics in power systems." , 1990 PhD diss., Virginia Tech.

[27] A.H.Nayfeh and D.T. Mook, Nonlinear Oscillations,1979, New York.

Contribution of individual authors to the creation of a scientific article (ghostwriting policy)

All authors contributed to the development of this paper.

Conceptualisation, Anastasia Sofroniou; Methodology, Anastasia Sofroniou and Bhairavi Premnath; Analytical and Numerical Analysis Bhairavi Premnath; Validation, Anastasia Sofroniou and Bhairavi Premnath; Writing-original draft preparation, Bhairavi Premnath and Anastasia Sofroniou; Writing-review and editing, All authors; Supervisors, Anastasia Sofroniou and Kevin J. Munisami.

Sources of Funding for Research Presented in a Scientific Article or Scientific Article Itself

No funding was received for conducting this study.

Conflict of Interest

The authors have no conflicts of interest to declare that are relevant to the content of this article.